

Energy migrations and transfers between Er^{3+} ions in Er_2SiO_5 films on SiO_2/Si substrates

Hiroo Omi^{1,2}

¹NTT Basic Research Laboratories, NTT Corporation,

²NTT Nanophotonics Center, NTT Corporation

Abstract : Optical energy migrations and transfers in erbium mono-silicate (Er_2SiO_5) grown on Si substrates by rf-magnetron sputtering are investigated by extended X-ray absorption fine structure (EXAFS) and time-resolved photoluminescence measurements. The energy transfer assisted by discrete excitation migration (hopping) among the Er^{3+} ions is evidenced by analyzing the lifetime of 1.5- μm photoluminescence from the erbium mono-silicate, for which interatomic distances between Er^{3+} ions have been precisely determined by EXAFS.

Keywords : Er, Extended x-ray absorption fine structure, Photoluminescence

Introduction

Erbium-doped materials, such as erbium silicates and erbium oxides, have received much attention as light emitters [1–3] and amplifiers [4] on silicon wafers at the telecommunications wavelength in silicon photonics. Erbium compounds such as Erbium silicates and erbium oxides themselves have a huge number of Er^{3+} ions of up to 10^{22} $1/\text{cm}^3$, which enables the fabrication of nanoscale optical waveguides and means they have great potential as nanoscale amplifiers on Si wafers. However, several types of poly crystals, mono-silicate (Er_2SiO_5), di-silicates ($\text{Er}_2\text{Si}_2\text{O}_7$), and their α -, β -, γ -type phases have been reported to form in the silicates, depending on the growth techniques, such as radio frequency (rf)-magnetron sputtering, and pulsed laser deposition, and substrates (*i.e.* Si or SiO_2/Si) [4–7]. The optical properties of erbium-doped materials strongly depend on the local structures of the crystals. For example, the distances between Er^{3+} – Er^{3+} ions in the crystal strongly govern the photoemission efficiencies. Of particular importance are that the energy migration between the Er^{3+} ions in the sili-

cate and energy transfers via Er^{3+} ions. The effect of energy migration has been actually demonstrated in a system of $\text{Er}_x\text{Y}_{2-x}\text{SiO}_5$ poly crystals [8]. Therefore, for better control of the optical properties, it is crucial to determine the crystal structure of the erbium silicates (*e.g.*, the distances between Er ions) and its relationship to the optical properties. However, despite their importance in silicon photonics [9, 10], the structures of the erbium silicates and their optical properties, especially the mechanism of energy migration, have not been established. In this work, we performed synchrotron X-ray absorption fine-structure experiments on erbium silicates grown by the rf-magnetron sputtering technique, which has been widely used for the fabrication of erbium silicates on 100-nm-thick SiO_2 film on Si wafers and subsequent thermal annealing at 1100°C in Ar gas ambient. We determined the crystal structure of erbium silicates and the distances between Er – Er ions in the erbium silicates. We also performed time-resolved photoluminescence (PL) measurements on the same samples. By combining the EXAFS results and time-resolved PL measurements, we clarified the mechanism of energy migrations and derived optical microparameters that govern PL quantum efficiency.

Experimental

The XAFS experiments were performed at beamline BL08B2 in SPring-8, Japan. The Er L_{III} -edge EXAFS spectra were collected at room temperature in the fluorescence mode. The fluorescence intensity was measured with a 19-element solid-state-detector (SSD). EXAFS spectra of Er_2O_3 crystalline powders were also collected in the transmission mode as standard references. The EXAFS data were analyzed using ATENA and ALTEMIS (ver. 6) packages. The 1.5- μm time-resolved PL measurements were performed at room temperature. A near-infrared streak camera was used for the detection of Er^{3+} emission from the samples for the time-resolved PL measurements [11]. The samples were pumped by a Ti: sapphire CW laser at 532-nm wavelength and a power of 30 mW. The erbium oxides were deposited on 100-nm-thick thermal $\text{SiO}_2/\text{Si}(100)$ wafers and subsequently annealed at 1100°C in Ar gas ambient.

Results and Discussion

Figure 1 shows the EXAFS spectra obtained from the sample annealed at 1100°C . In the radial profiles [Fig. 1(a)], we can see two main peaks at 0.2 and 0.3 nm. Theoretical best fittings are also shown in Figs. 1(a) and (b) as red solid lines. As can be seen in Figs. 1(a) and (b), the experimental profiles are in good agreement with the simulations (R factor = 0.0444). The best fits are obtained for the mono-silicate of Er_2SiO_5 when the atomic positions of Y_2SiO_5 (JCPDS card: No. 52-1810) are used instead as initial parameters for the fittings. Note here that we assume the atomic positions of Y, Si, and O in Y_2SiO_5 as those of Er, Si, and O in Er_2SiO_5 for the profile fittings, since the atomic positions of Er_2SiO_5 (JCPDS card: No. 40-384) have not been precisely determined at present. The assumption is validated by the facts that the ionic radius of Er and Y are almost same (Er: 0.89\AA , Y: 0.9\AA) and unit cells and that the lattice constants of Er_2SiO_5 are almost the same as those of Y_2SiO_5 . As a reference, we also simulated an EXAFS profile

of erbium di-silicate (Er_2SiO_7) (JCPDS card: No. 48-1595), where atomic positions have been determined, but it does not well fit the experimental result. From the agreement of the fittings with the mono-silicate, we can say that the thermal annealing produces the mono-silicate of Er_2SiO_5 (JCPDS card 40-384) through the interface reaction between Er_2O_3 and SiO_2 , which enables us to determine the distances between Er - O ions and between Er - Er ions in the Er_2SiO_5 crystals. The interatomic distances R and Debye-Waller disorder factors σ^2 are summarized in Table 1. The Debye-Waller disorder factors σ^2 are compatible with those of Er_2O_3 crystal [9], suggesting the good crystalline quality of the mono-silicate formed by thermal annealing at 1100°C .

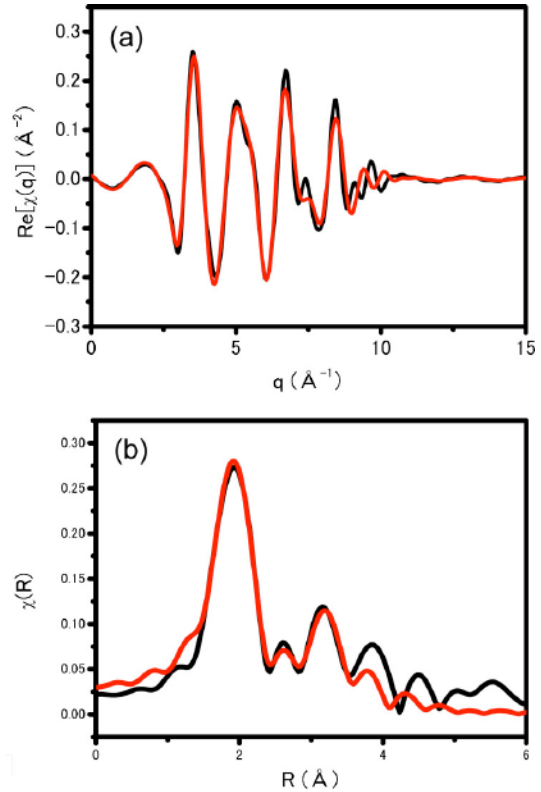


Fig. 1. Er L_{III} -edge EXAFS spectrum of Er^{3+} in the sample. Red solid line is the fitting by the theory. χ , R , and q represent X-ray absorption, distance, and wavenumber, respectively. (b) Fourier-transformed XAFS spectrum of the sample (see Table 1 for details).

Table 1. Interatomic distances (R) of Er – O, Er – Si and Er – Er in the unit cell up to 3.5Å and the Debye-Waller disorder factor (σ^2), determined by EXAFS. The suffixes represent the different sites of O and Er atoms in the unit cell.

	$R(\text{Å})$	$\sigma^2(\text{Å}^2)$
Er1-O1	2.2551	0.0141
Er1-O2	2.2702	0.0539
Er1-O3	2.2866	0.0629
Er1-O4	2.2937	0.0024
Er1-O5	2.3074	0.0724
Er1-O6	2.7754	0.0147
Er1-O7	3.1132	0.0142
Er1-Si	3.292	0.0155
Er1-Er1	3.4565	0.0148
Er1-Er2	3.4972	0.009

Figure 2(a) shows the PL spectrum obtained from the sample. It is evident that there are a main peak at 1528.8 nm, which is the transition between ${}^4I_{13/2}(X_1) - {}^4I_{15/2}(Z_1)$ states of $4f$ -levels of Er^{3+} ions in Er_2SiO_5 films, and some additional peaks due to Stark splitting. The shape and positions of the PL are in good agreement with previous results [4]. The decay profile of the peak and the corresponding $\ln(-\ln(t/\tau_R) - t/\tau_R - (\ln(t/\tau_R))^3)$ plots are shown in Fig. 2(b) and the inset, respectively, where τ_R is the intrinsic fluorescence decay time of the donor. According to the Inokuti-Hirayama (I-H) equation [12], the slope of the plots in the inset corresponds to $3/s$, where s is multipole interaction parameter ($s = 6, 8,$ and 10 for dipole-dipole, dipole-quadrupole, and quadrupole-quadrupole interactions). From the slope in the inset, we obtained $s = 4.4$, which is fairly close to $s = 6$, indicating that the energy transfer is caused by the dipole-dipole interactions between Er^{3+} ions. It can be seen, however, that the experimental plots are not completely in agreement with the I-H equation; they deviate for shorter and longer decay time ranges. This could be because the energy transfer from donors to acceptors is assisted by energy migration among donors due to the

high concentration of Er^{3+} ions in the mono-silicate, as described below.

Figure 2(b) shows the decay curve of the peak at 1528 nm from the Er_2SiO_5 film grown on Si(100). As seen in this figure, the experimental curve decays non-exponentially and agrees well with the simulation on the basis of the model in which energy transfer is accelerated by energy migration through hopping proposed by Burshtein [13]. In the hopping model, PL intensity $I(t)$ can be expressed $I(t) = I_0 \exp(-t/\tau_R - \gamma t^{1/2} - Wt)$, where τ_R is the intrinsic radiative lifetime of erbium ions, γ is the donor-to-acceptor energy transfer parameter (direct transfer without migration), W is the rate parameter related

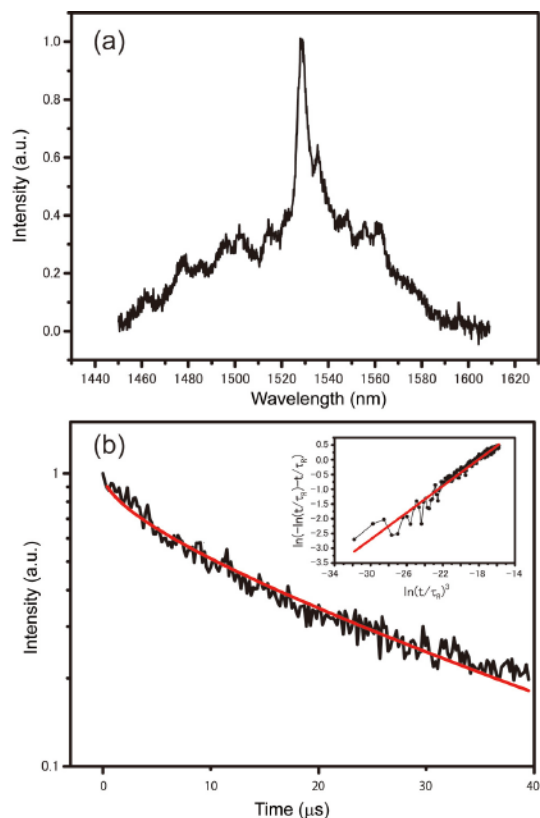


Fig. 2. (a) PL spectrum obtained from the sample. (b) Normalized decay curve of ${}^4I_{13/2}(X_1) - {}^4I_{15/2}(Z_1)$ emission under pulsed excitation for the Er_2SiO_5 . The red solid line is the theoretical fit by the Burshtein equation. Inset shows the $\ln(-\ln(t/\tau_R) - t/\tau_R - (\ln(t/\tau_R))^3)$ plot of the decay curve in (b).

to the donor-to-acceptor energy transfer assisted by discrete excitation migration (hopping) among donor states. In this case, the energy transfer is referred to as migration-accelerated. From the theoretical fitting, we obtained $\gamma = 150.4$ with standard errors (SE) of $12.7 \text{ s}^{1/2}$ and $W = 19172.4$ with $SE = 2910.2 \text{ s}^{-1}$ at $\tau_R = 7.4 \text{ ms}$ [14]. Subsequently, the microparameters of energy transfer from donor to acceptor C_{DA} and that from donor to donor C_{DD} can be estimated from the value of γ and W by the following relationships [15–17]: $\gamma = \frac{4}{3}\pi^{3/2}N_A\sqrt{C_{DA}}$, $W = K_h = \pi\left(\frac{2}{3}\pi\right)^{5/2}N_A N_D\sqrt{C_{DA}C_{DD}}$, $K_d = [16\pi^2/(3 \times 2^{3/4})]N_A N_D C_{DA}^{1/4} C_{DD}^{3/4}$, where N_A and N_D are the concentration of acceptors and donors in the erbium mono-silicate, and K_d is the energy transfer rate, which is associated with diffusion and trapping derived from the random walk treatment. We obtained $C_{DA} = 1.94 \times 10^{-42} \text{ cm}^6/\text{s}$ and $C_{DD} = 3.74 \times 10^{-42} \text{ cm}^6/\text{s}$, which lead to the critical radii $R_{DA} = 4.95\text{\AA}$ and $R_{DD} = 6.03\text{\AA}$, and hopping time $t_h = 81.6 \mu\text{s}$. The critical radii indicate that the energy transfer and migration can occur among ions located within these distances. The rates of cross-relaxation (P_{DA}) and that of energy migration (P_{DD}) are estimated to be 132 and 78 s^{-1} , respectively, using the equations $P_{DA} = C_{DA}/R_{DA}^6$ and $P_{DD} = C_{DD}/R_{DD}^6$. According to Ref. 17, S is a good indicator for distinguishing the migration mechanisms, where $S = W/K_d$. Owing to this criteria, the diffusion mechanism satisfies $S = 1$ independent of the value of C_{DD}/C_{DA} [16] and the hopping mechanism works for $S < 1$ [13], depending on C_{DD}/C_{DA} . From the fitting, we obtained $S = 0.544$ and $C_{DD}/C_{DA} = 3.25$, indicating that energy migration is due to energy hopping between Er^{3+} ions [see Fig. 6 in Ref. 17], but not due to the diffusion-limited mechanism where $S = 1$. Furthermore, when we plot our result on Fig. 6 in Ref. 17, we find that the plot rides on the solid curve of that figure. This indicates that the hopping mechanism of our system is in good accordance with the modified hopping model proposed by Jagosich *et al.*

(Ref. 17), in which exciton trapping efficiency is taken into account. Note that, on the other hand, the diffusion-limited mechanism has been suggested in the $\text{Er}_x\text{Y}_{x-2}\text{SiO}_5$ ($0.06 \leq x \leq 2$) crystals [6], which is not in accordance with the results described above.

Regarding R_{DA} , the distance is nearly equal to the average Er – Er ions distance of $R_{\text{Er-Er}} = 4.6\text{\AA}$, which is derived from the EXAFS analysis, indicating that the energy transfer is mainly caused by cross-relaxations between Er^{3+} ions, such as cooperative up-conversions. Actually, evidence of such up-conversions has been found in waveguides of polycrystalline $\text{Er}_x\text{Y}_{x-2}\text{SiO}_5$ films grown on Si covered with thermal oxide films by ion-beam sputtering [18]. Additionally, we derived the average lifetime by normalizing to unity the PL decay curve at time $t = 0$ and integrating over the entire decay curve for non-exponential decay according to the expression $\tau_{eff} = \int_0^\infty I(t)/I_0 dt$, in which I_0 is the PL intensity at $t = 0$. We obtained $\tau_{eff} = 15.95 \mu\text{s}$, which is nearly equal to the value obtained by Miritello *et al.* [6]. The relative quantum efficiency η is estimated to be 0.21% by the equation $\eta = \tau_{eff}/\tau_R$.

Conclusion

In conclusion, we have investigated the optical energy transfers and energy migrations between Er^{3+} ions in Er_2SiO_5 grown on SiO_2/Si substrates by rf magnetron sputtering and subsequent thermal annealing at 1100°C in Ar gas ambience. We determined the local structures of Er_2SiO_5 (JCPDS card: No.40-384) by EXAFS and quantitatively clarified from time-resolved PL measurements that the energy migrations between Er^{3+} ions in the mono-silicate can be explained by the modified Burshtein’s hopping model and that the energy transfers are possibly due to cooperative up-conversions between Er^{3+} ions in the Er_2SiO_5 film on Si.

事業への貢献

光情報通信事業に革新をもたらすエルビウム添加発光材料の開発に貢献する。

References

- [1] F. Iacona, G. Franzo, M. Miritello, R. L. Savio, E. F. Pecora, A. Irrera, and F. Priolo, *Opt. Mater.* **31**, 1269 (2009).
- [2] Y. Yin, W. J. Xu, G. Z. Ran, G. G. Qin, S. M. Wang, and C. Q. Wang, *J. Phys. Condens. Matter.* **21**, 012204 (2009).
- [3] A. Pan, L. Yin, Z. Liu, M. Sun, R. Liu, P. L. Nichols, Y. Wang, and C. Z. Ning, *Opt. Mater. Express* **1**, 1202 (2011).
- [4] H. Isshiki, *IEICE Trans. Electron.* **E91**, 138 (2008).
- [5] R. L. Savio, M. Miritello, A. M. Piro, F. Priolo, and F. Iacona, *Appl. Phys. Lett.* **93**, 021919 (2008).
- [6] M. Miritello, R. L. Savio, F. Iacona, G. Franzo, A. Irrera, A. F. Piro, C. Bongiorno, and F. Priolo, *Adv. Mater.* **19**, 1582 (2007).
- [7] X. J. Wang, T. Nakajima, H. Isshiki, and T. Kimura, *Appl. Phys. Lett.* **95**, 041906 (2009).
- [8] T. Nakajima, T. Kimura, and H. Isshiki, *Extended abstract for the International Conference of Solid State Devices and Materials (SSDM) 2010*, 427 (2010).
- [9] T. T. Van, J. R. Bargar, and J. P. Chang, *J. Appl. Phys.* **100**, 023115 (2006).
- [10] N. D. Afify, G. Dalba, C. Armellini, M. Ferrari, Rocca, and A. Kuzmin, *Phys. Rev. B* **76**, 024114 (2007).
- [11] H. Omi and T. Tawara, *Jpn. J. Appl. Phys.* **51**, 02BG07/1-3 (2012).
- [12] M. Inokuti and F. Hirayama, *J. Chem. Phys.* **43**, 1978 (1965).
- [13] A. I. Burshtein, *Sov. Phys. JETP* **35**, 882 (1972).
- [14] J. H. Shin, M.-S. Yang, J.-S. Chang, S.-Y. Lee, K. Suh, H. G. Yoo, Y. Fu, and P. Fauchet, *Proc. SPIE* **6897**, 68970N (2008).
- [15] B. Henderson and C. F. Imbusch, *Optical Spectroscopy of Inorganic Solids* (Oxford Univ. Press, New York, USA, 1989) p. 445.
- [16] M. Yokota and O. Tanimoto, *J. Phys. Soc. Jpn.* **22**, 779 (1967).
- [17] F. H. Jagosich, L. Gomes, L. V. G. Tarelho, L. C. Courrol, and I. M. Ranieri, *J. Appl. Phys.* **91**, 624 (2004).
- [18] K. Suh, M. Lee, J. S. Chang, H. Lee, N. Park, G. Y. Sung, and J. H. Shin, *Opt. Express* **18**, 7724 (2010).